Author for correspondence:
Franz Conen
e-mail: franz.conen@unibas.ch

THE ROYAL SOCIETY PUBLISHING

Export of ice-nucleating particles from watersheds: results from the Amazon and Tocantins river plumes

Annika Einbock, Emma Burtscher, Claudia Frey and Franz Conen

Department of Environmental Sciences, University of Basel, Bernoullistrasse 30, 4056 Basel Switzerland

FC, 0000-0003-4821-5775

We examined ice-nucleating particles (INPs) in the plumes of the Tocantins and Amazon rivers, which drain watersheds with different proportions of degraded land. The concentration of INPs active at $-15°C$ (INP_{-15}) was an order of magnitude lower in the Tocantins (mean $= 13.2\ ml^{-1}$; s.d. $= 7.8\ ml^{-1}$), draining the more degraded watershed, compared with the Amazon (mean $= 175.8\ ml^{-1}$; s.d. $= 11.2\ ml^{-1}$), where the concentration was also significantly higher than in Atlantic surface waters (mean $= 3.2\ ml^{-1}$; s.d. $= 2.3\ ml^{-1}$). Differences in heat tolerance suggest that INPs emitted by the Amazon rainforest to the atmosphere or washed into the river might originate from contrasting sources on top of and below the rainforest canopy, respectively. For the Amazon River, we estimate a daily discharge of 10^{18} INP_{-15} to Atlantic waters. Rivers in cooler climate zones tend to have much higher concentrations of INPs and could, despite a smaller water volume discharged, transfer even larger absolute numbers of INP_{-15} to shelf waters than does the Amazon. To what extent these terrestrial INPs become aerosolized by breaking waves and bubble-bursting remains an open question.

1. Introduction

Ice-nucleating particles (INPs) are a prerequisite for initial ice formation in clouds at temperatures warmer than $-38°C$ [1,2]. Ice is the starting point for most precipitation above continents [3]. Land and ocean both emit INPs, but ice-nucleation active site densities in sea-surface aerosols are a few orders of magnitude lower than in continental boundary layer aerosols [4]. Some rivers have been reported to carry high concentrations of INPs that have been
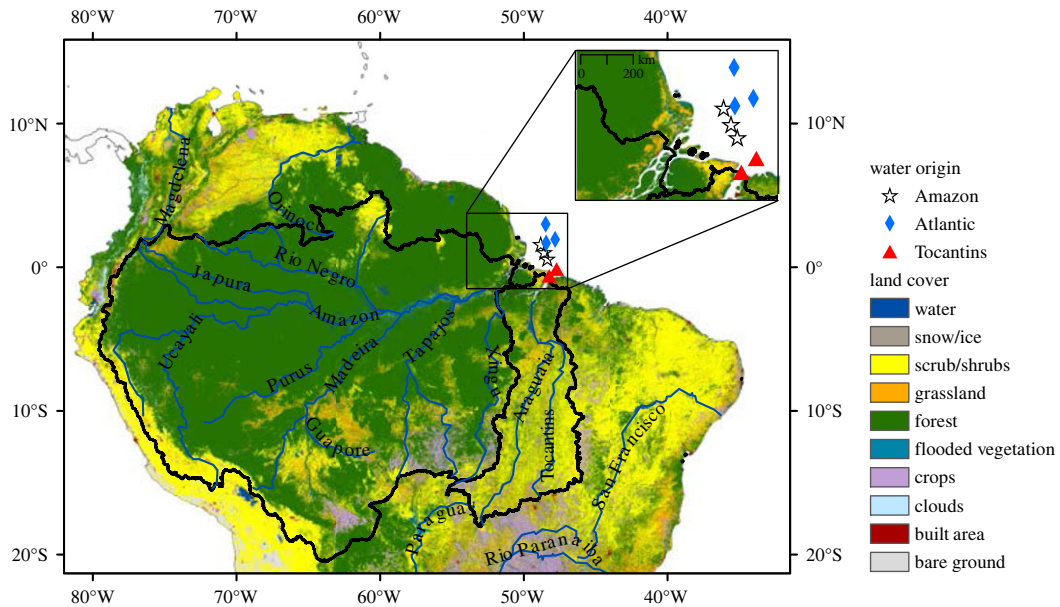
Figure 1. Land cover (100 × 100 m resolution) in the watersheds of the Amazon River (large, western area bordered by black line) and the Tocantins River (smaller, eastern area bordered by black line). Sampling locations in the Amazon (white stars) and Tocantins (red triangles) river plumes, and in the Atlantic (blue diamonds). Sources: Land cover: Sentinel-2, 2020, resampled at 100 m resolution (https://www.arcgis.com/apps/instant/media/index.html?appid=fc92d38533d440078f17678ebc20e8e2); watersheds: Agência Nacional de Águas e Saneamento Básico (ANA) (https://metadados.snirh.gov.br/geonetwork/srv/search?keyword=Ottobacia).

produced on land rather than in the river itself [5–9]. When discharged to the ocean, they probably enhance INP concentration at the surface of shelf waters, possibly creating source areas from where INPs of marine and terrestrial origins are aerosolized in parallel by wave-breaking and bubble-bursting. Earlier work on the number of biological INPs produced by decaying leaves has suggested that biological INP production on land may increase by orders of magnitude successively from tropical to temperate to cold climate zones [10,11]. Further, different INP densities are observed on contrasting types of vegetation, where land-use change is suspected to modify INP sources and thereby the formation of precipitation [12].

Perhaps, the study of INPs in rivers draining watersheds with different land cover can reveal effects of land-use change on INP production and, subsequently, on the atmospheric hydrological cycle [12,13]. Here, we report on INPs in the plumes of the Amazon and Tocantins rivers. The Amazon River drains the largest watershed worldwide and has an annual average flow rate at the Óbidos station of 150 500 $m^3 s^{-1}$ [14]. The watershed of the Tocantins River is about six times smaller and its average discharge at the Tucurui station is about 13 times smaller [15] than the Amazon. Seasonal changes in rainfall [15] are reflected in discharge, which in the Amazon ranges from approximately 100 200 to 240 000 $m^3 s^{-1}$ [14].

A much larger fraction of the Tocantins watershed has deteriorated due to deforestation and drought over the past decades than is the case for the Amazon watershed [16]. Unlike the Amazon, the Tocantins watershed also includes dryer climate types. Thus, effects of land-use change cannot be separated from climate effects. However, both climate change and deforestation are expected to lead to drier conditions in the Amazon region [17]. Therefore, INPs in the Tocantins watershed today might be a proxy for what they might become in the Amazon watershed in future. We expected differences in land cover between both watersheds to result in different INP populations in the plumes of the Amazon and Tocantins rivers. These differences should emerge primarily in INPs active at −15°C or above (INP$_{-15}$), because most INP$_{-15}$ are of biological origin and are ultimately derived from plants and associated microorganisms [18–20].

2. Material and methods

2.1. Land cover in the Amazon and Tocantins watersheds

Currently, the majority of the Amazon River watershed is covered by forest (81%), followed by scrub and shrubs (10%) (figure 1). Grassland (4%) and crops (3%) cover a smaller proportion than in the Tocantins

Table 1. Origin of samples analysed for their content of INPs and properties of the sampled waters.

origin of water	sample no.	date	time (UTC)	latitude	longitude	conductivity (mS cm^{-1})	salinity (PSU)	fluorescence (mg m^{-3})	turbidity (NTU)
Tocantins	1	23.04.2021	07:23	00°07.30′ S	047°43.87′ W	7.5	3.9	1.1	5.3
	2	23.04.2021	15:54	00°35.85′ S	048°14.63′ W	2.0	0.9	1.1	9.7
Amazon	3	24.04.2021	12:57	00°35.83′ N	048°22.40′ W	1.1	0.5	1.0	9.7
	4	24.04.2021	16:07	01°02.91′ N	048°35.18′ W	1.6	0.7	1.1	9.7
	5	24.04.2021	00:48	01°36.73′ N	048°50.29′ W	6.4	3.2	1.2	3.2
Atlantic	6	29.04.2021	07:40	03°00.15′ N	048°28.91′ W	57.3	35.1	0.09	0.08
	7	30.04.2021	16:09	04°24.35′ N	049°07.29′ W	57.4	36.0	0.22	0.08
	8	03.05.2021	20:00	05°02.01′ N	050°21.12′ W	57.5	35.6	0.08	0.08

River watershed (9% and 7%, respectively), where the share of forest is only 36%, and scrub and shrubs are more abundant (45%) (figure 1).

2.2. Field sampling

Water was sampled towards the end of the rainy season from the plumes of the Amazon River and the Tocantins River during the cruise M174 of the research vessel R/V *Meteor* [21]. The focus of the cruise was on exploring the fate of nitrogen in the Amazon River plume and the western tropical North Atlantic [22]. Surface water pumped from the moon pool, an opening in the base of the hull 5.70 m below the water line, was collected in sterile polypropylene tubes (40 ml). To prevent eventual contamination with residues in the pumping system, the water was kept running for several minutes beforehand. Samples were immediately put into a −20°C freezer and remained frozen until analysis. High-resolution data on water quality was collected with the CTD-system 'SBE 911plus' (SN-0603, SEABIRD-ELECTRONICS, USA), with added sensors to measure pressure, temperature (2× SBE 3), conductivity (2× SBE 4), oxygen concentration (2× SBE 43), chlorophyll-a fluorescence (683 nm), turbidity, PAR, SPAR and nitrate (SUNA sensor).

Salinity data confirms that samples collected at the mouths of the Amazon and Tocantins rivers were indeed river water with little or no seawater (table 1). The fluorescence values were practically the same in both river plumes. Turbidity was lower by a factor of two or three in one sample from the Amazon River and one from the Tocantins River plume. Both of these samples also had a slightly enhanced salinity.

2.3. Analysis of INPs

Immediately after melting a sample at room temperature, we transferred a subsample of 100 µl in each of 52 Eppendorf safe-lock tubes (0.5 ml) for analysis on the ice-nucleation detection apparatus described in Stopelli *et al.* [23]. Tubes were cooled at a rate of 0.3°C min^{-1} from 0 to −20°C. The freezing temperature of the subsample in each tube was detected automatically and the cumulative INP concentration at every 0.5°C step was calculated according to Vali [24]. When all 52 droplets had frozen before reaching −12°C, we reanalysed samples in a 1:10 dilution with ultrapure water (Sigma-Aldrich, W4502-1L) to extend the measurement range to −15°C. Duplicate blank tests with only ultrapure water confirmed it was free of INP$_{-15}$. For characterizing INPs in terms of their heat sensitivity, we performed the same freezing assay two more times: after treating the same array of subsamples in their Eppendorf tubes for 10 min in a water bath at 60°C and after a second such treatment at 95°C. In the Atlantic water samples, we shifted measured values by 2°C towards the warmer end of the temperature scale to account for freezing depression due to high salt concentration. We derived the 2°C value from the difference between freezing spectra with Snomax in pure water and with Snomax in pure water to which we added an equivalent of 35 g l^{-1} NaCl.

3. Results and discussion

Cruise M174 gave us the opportunity to take a snapshot of INPs in a region we otherwise could not have accessed. The sampled river plumes integrate diversity and variation of innumerous watercourses that
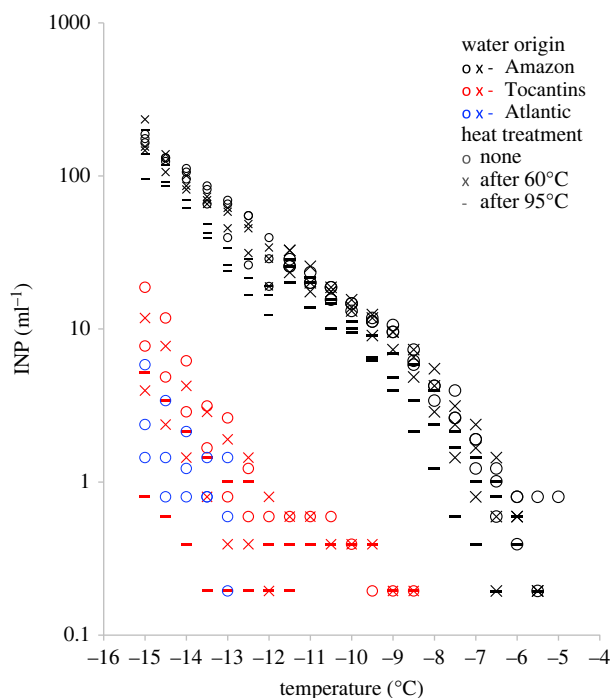
Figure 2. Concentration of INPs active between −5 and −15°C in three samples of the Amazon River plume (black), two samples of the Tocantins River plume (red) and three samples of Atlantic surface water (blue). The Atlantic samples, all containing more than 35 g salt l^{-1}, were adjusted for freezing point depression. We analysed the same sample material three times: first, without any treatment (circles); second, after heating to 60°C (cross symbols); and third, after heating to 95°C (dash symbols). In addition, we analysed Amazon River plume samples in a 10-fold dilution with pure water (smaller symbols) to determine INP concentration at lower temperatures than was possible with undiluted samples (data in electronic supplementary material).

supply the Tocantins and Amazon rivers before they reach the Atlantic. Successive integration of distant tributaries with asynchronous variation within a large watershed confers a relative stability in terms of biotic and abiotic properties to the water discharged to the ocean [25]. Therefore, we expect our investigation to afford meaningful interpretation despite its snapshot character and the small number of samples.

3.1. Concentration of INPs in river plumes

The onset of freezing in 1 ml of water was observed at −6.5°C in the Amazon River plume and at −12.5°C in the Tocantins River plume. Differences between samples taken from within the same river plume were small (figure 2). The number of INP$_{-15}$ in 1 ml of water was one order of magnitude higher in the Amazon River plume (mean = 175.8; s.d. = 11.2) than the Tocantins River plume (mean = 13.2; s.d. = 7.8). While this difference was statistically significant ($p < 0.001$), the difference between the Tocantins River plume and Atlantic surface water (mean = 3.2; s.d. = 2.3) was much smaller and statistically insignificant ($p = 0.31$). From the annual average flow rate of both rivers and the concentration difference between their plumes and Atlantic surface water, we estimate a net daily discharge in the order of 10^{18} INP$_{-15}$ for the Amazon and 10^{16} INP$_{-15}$ for the Tocantins.

A substantial fraction of INPs found in river water pass through a 0.22 µm filter [5–8]. In a limnological context, these small INPs would be referred to as dissolved organic matter (DOM). The quality of DOM in rivers clearly depends on land cover in the watershed area [26], which might explain some of the difference in INPs between the Tocantins and Amazon. The 10^1 and 10^2 INP$_{-15}$ ml^{-1} in the Tocantins and the Amazon rivers, respectively, were three and two orders of magnitude lower than what has been reported from the lower reaches of the Mississippi River [7], the largest river in North America. Interestingly, the difference in INP$_{-15}$ on decaying leaves from tropical and temperate regions is of the same direction and order of magnitude [10]. Therefore, despite an about tenfold smaller discharge, the Mississippi River might still transfer an order of magnitude more INPs from land to ocean than does the Amazon. Mississippi freshwater influences substantial areas in the northern Gulf of Mexico [27], where discharged INPs could become aerosolized by wave-breaking

Table 2. Fraction of INPs active between −13 and −15℃ by category of heat sensitivity. The fraction of INPs lost in the 60℃ treatment is termed heat sensitive; the fraction tolerating 60℃ but deactivated by 95℃ is termed moderately heat tolerant; and the fraction still active after both treatments is called heat tolerant. Mean values are for five measurement points on three and two samples from the Amazon and Tocantins river plumes, respectively (s.d. = standard deviation).

category of INPs	Amazon		Tocantins	
	mean	s.d.	mean	s.d.
heat sensitive	0.06	0.16	0.39	0.14
moderately heat tolerant	0.29	0.14	0.36	0.05
heat tolerant	0.66	0.18	0.25	0.13

and bubble-bursting [28,29], as are INPs of marine origin in the Gulf of Mexico [30], perhaps with atmospheric implications. For example, at their coastal observatory in Yucatan, Ladino *et al.* [31] found an enhanced atmospheric concentration of INP_{-15} in marine air masses arriving with two cold fronts from northerly directions. Also in other regions, shelf waters enriched with INPs from large rivers could be an atmospherically relevant source of INPs to marine air masses. Furthermore, the origin of highly active INPs in the atmosphere above the North Pole has been traced back to the region of shallow waters over the Russian continental shelf [32]. Unfortunately, the INP concentration in Siberian rivers feeding these shelf waters is still unknown, but the analyses by Schnell & Vali [10,11] on decaying leaves from different climatic zones suggest even higher INP concentrations in the Siberian rivers than in rivers in temperate regions. In addition, thawing permafrost in Siberian river catchments probably adds further INPs that are discharged into shelf waters of the Arctic Ocean [33].

3.2. River water and the atmosphere can have different sources of INPs

The concentration of INPs was different between the two river plumes, as was the pattern of heat sensitivity in these INPs, although other parameters known to drive INP concentration—such as turbidity [8] and humic-like substances [34], of which fluorescence is a measure—were similar in both river plumes (table 1).

Typically, heat tolerance of INPs decreases markedly with increasing activation temperature, whether in soil [18,35], air [36–38], precipitation [37,39] or seawater [40,41]. Therefore, in the following we focus on a temperature window from −13 to −15℃ and average all measurements made in 0.5℃ steps within this window.

In the Tocantins water, 39% of all INPs were heat sensitive and only 25% were heat tolerant (table 2). In the Amazon water, few INPs were heat sensitive but 66% were heat tolerant. This fraction is nearly four times as large as the heat-tolerant fraction of INPs in airborne particles above the middle of the Amazon rainforest (18%, s.d. = 15%; derived from values in fig. 6 in [38]). An explanation for this discrepancy could be that INPs in the air above dense canopies and INPs in water below them are from separate and contrasting sources. Seven-day back trajectories indicate that air masses above the canopy had arrived from the Atlantic and crossed the coastline near the mouths of the Amazon and Tocantins rivers before reaching the air-sampling location about 1200 km further inland [38]. If the air masses contained INPs from the Amazon River plume, their signature in terms of heat sensitivity could have been unrecognizably diluted by further INPs taken up during the 1200 km journey westward over the Amazon rainforest.

During the rainy season, when samples were taken, much of the DOM in river water probably originates from compounds washed from litter and soil into the river [42], whereas aerosol particles above the canopy more likely are emitted from the canopy itself. When raindrops impinge on leaves and branches, they generate aerosols containing microorganisms from these surfaces. Driving mechanisms can involve bubble-bursting at the surface of water films by which tiny droplets (10–100 μm) and particles are aerosolized [43]. Other possibilities of aerosol generation by rain impact on canopies include micro-splashing [44]. Droplets thus produced can be smaller than 50 μm [45] and get lofted above a canopy [46], where they evaporate in the drier air [47] and enrich it with the INPs [48,49] that were initially contained in the splash droplets. Whatever the mechanism, the most likely source of INPs aerosolized by raindrops impinging on the canopy would be ice-nucleation active

epiphytic microorganisms, most of which are heat sensitive and only some are moderately heat tolerant [20]. Heat-sensitive INPs washed by rain from canopies will mix on the ground with a probably much larger pool of INPs that themselves are very unlikely to be transported through and above the canopy of the tropical rainforest. At night, the air below the canopy is persistently decoupled from that above it [50,51]. During the daytime, larger turbulent structures may occasionally penetrate the dense foliage of the canopy and result in an occasional exchange of air and particles. However, observations of fluorescent biological aerosol particles above and below a rainforest canopy in Borneo have suggested only a weak coupling of larger aerosol particles between these layers [52]. Known heat-tolerant INPs that could be washed from litter and soil into the river are mineral particles [53], lignin [54] and other heat-stable organics [9,36], such as macromolecules of pollen [55]. A much stronger source of such heat-tolerant INPs below the canopy in the Amazon compared with the Tocantins watershed would explain (i) the greater abundance of INPs in the Amazon, (ii) the larger fraction of heat-tolerant INPs in the Amazon compared with the Tocantins River plume, and (iii) the difference in heat-tolerant fraction between INPs in the river plume and INPs in the air above the Amazon rainforest.

4. Conclusion

To conclude, land-use change probably affects the abundance and composition of INPs washed into watercourses. Although INPs might be produced at higher rates where rainforests are less degraded, the dense canopies of intact rainforests probably obstruct the stronger sources from emitting to the atmosphere. Therefore, the difference in INP concentration and heat-tolerance in the two investigated river plumes is unlikely to translate to similar differences in INPs emitted directly from their watersheds to the atmosphere above. Nevertheless, INPs discharged by the Amazon River into the Atlantic significantly increase the INP concentration in water above the continental shelf and could affect the INP concentration and composition in marine air masses. Although the Amazon is the largest river in terms of discharge, smaller rivers in temperate or cold regions might transfer even more INPs to shelf waters, because decaying leaves are a stronger source of INPs in colder climates than in a tropical climate. Variations in atmospheric INP concentration reported from the Gulf of Mexico and the Arctic Ocean lend initial support to the idea that INPs transported by large rivers from land to shelf waters could have a discernible impact on the atmospheric INP concentration in marine air masses.

References

1. Findeisen W. 1938 Die kolloidmeteorologischen Vorgänge bei der Niederschlagsbildung (Colloidal meteorological processes in the formation of precipitation). *Meteorol. Z.* **55**, 121–133. (translated and edited by Volken E, Giesche AM, Brönnimann S. 2015 *Meteorol. Z.*, **24** (doi:10.1127/metz/2015/0675)

2. Kanji ZA, Ladino LA, Wex H, Boose Y, Burkert-Kohn M, Cziczo DJ, Krämer M. 2017 Overview of ice nucleating particles. *Meteorol. Monogr.* **58**,

1.1–1.33. (doi:10.1175/AMSMONOGRAPHS-D-16-0006.1)

3. Mülmenstädt J, Sourdeval O, Delanoë J, Quaas J. 2015 Frequency of occurrence of rain from liquid-, mixed-, and ice-phase clouds derived from A-Train satellite retrievals. *Geophys. Res. Lett.* **42**, 6502–6509. (doi:10.1002/2015GL064604)

4. DeMott PJ *et al.* 2015 Sea spray aerosol as a unique source of ice nucleating particles. *Proc.*

Natl Acad. Sci. USA **113**, 5797–5803. (doi:10.1073/pnas.1514034112)

5. Moffett BF. 2016 Fresh water ice nuclei. *Fundam. Appl. Limnol.* **188**, 19–23. (doi:10.1127/fal/2016/0851)

6. Larsen JA, Conen F, Alewell C. 2017 Export of ice nucleating particles from a watershed. *R. Soc. Open Sci.* **4**, 170213. (doi:10.1098/rsos.170213)

7. Moffett BF, Hill TCJ, DeMott PJ. 2018 Abundance of biological ice nucleating particles

in the Mississippi and its major tributaries. *Atmosphere* **9**, 307. (doi:10.3390/atmos9080307)

8. Knackstedt A *et al.* 2018 Terrestrial origin for abundant riverine nanoscale ice-nucleating particles. *Environ. Sci. Technol.* **52**, 12 358–12 367. (doi:10.1021/acs.est.8b03881)

9. Borduas-Dedekind N, Ossola R, David RO, Boynton LS, Weichlinger V, Kanji ZA, McNeill K. 2019 Photomineralization mechanism changes the ability of dissolved organic matter to activate cloud droplets and to nucleate ice crystals. *Atmos. Chem. Phys.* **19**, 12 397–12 412. (doi:10.5194/acp-19-12397-2019)

10. Schnell RC, Vali G. 1973 Worldwide souce of leaf derived freezing nuclei. *Nature* **246**, 212–213. (doi:10.1038/246212a0)

11. Schnell R, Vali G. 1976 Biogenic ice nuclei: part I. Terrestrial and marine sources. *J. Atmos. Sci.* **33**, 1554–1564. (doi:10.1175/1520-0469(1976)033<1554:BINPIT>2.0.CO;2)

12. Morris CE, Conen F, Huffman JA, Phillips V, Pöschl U, Sands DC. 2014 Bioprecipitation: a feedback cycle linking earth history, ecosystem dynamics and land use through biological ice nucleators in the atmosphere. *Glob. Change Biol.* **20**, 341–351. (doi:10.1111/gcb.12447)

13. Sheil D. 2018 Forests, atmospheric water and an uncertain future: the new biology of the global water cycle. *For. Ecosyst.* **5**, 19. (doi:10.1186/s40663-018-0138-y)

14. Espinoza Villar JC *et al.* 2009 Contrasting regional discharge evolutions in the Amazon basin (1974–2004). *J. Hydrol.* **375**, 297–311. (doi:10.1016/j.jhydrol.2009.03.004)

15. García NO, Mechoso CR. 2005 Variability in the discharge of South American rivers and in climate / Variabilité des débits de rivières d'Amérique du Sud et du climat. *Hydrol. Sci. J.* **50**, null–478. (doi:10.1623/hysj.50.3.459.65030)

16. Bullock EL, Woodcock CE, Souza Jr C, Olofsson P. 2020 Satellite-based estimates reveal widespread forest degradation in the Amazon. *Glob. Chang. Biol.* **26**, 2956–2969. (doi:10.1111/gcb.15029)

17. Swann LS, Longo M, Knox RG, Lee E, Moorcroft PR. 2015 Future deforestation in the Amazon and consequences for South American climate. *Agric. For. Meteorol.* **214–215**, 12–24. (doi:10.1016/j.agrformet.2015.07.006)

18. Hill TCJ, DeMott PJ, Tobo Y, Fröhlich-Nowoisky J, Moffett BF, Franc GD, Kreidenweis SM. 2016 Sources of organic ice nucleating particles in soils. *Atmos. Chem. Phys.* **16**, 7195–7211. (doi:10.5194/acp-16-7195-2016)

19. Testa B *et al.* 2021 Ice nucleating particle connections to regional Argentinian land surface emissions and weather during the Cloud, Aerosol, and Complex Terrain Interactions experiment. *J. Geophys. Res Atmos.* **126**, e2021JD035186. (doi:10.1029/2021JD035186)

20. Conen F, Einbock A, Mignani C, Hüglin C. 2022 Measurement report: ice nucleating particles active ≥−15°C in free tropospheric air over western Europe. *Atmos. Chem. Phys.* **22**, 3433–3444. (doi:10.5194/acp-22-3433-2022)

21. Voss M. 2021 Master tracks in different resolutions of METEOR cruise M174, Las Palmas - Emden, 2021-04-12 - 2021-05-29. *PANGAEA Digital Repository*. (doi:10.1594/PANGAEA.935041)

22. Voss M *et al.* 2021 Nitrogen cycling and physical processes in the Amazon River plume, Cruise No. M174, 12/04/2021–30/05/2021, Las Palmas (Spain) - Emden (Germany). *METEOR-Berichte* **M174**, 1–40. (https://doi.org/10.48433/cr_m174)

23. Stopelli E, Conen F, Zimmermann L, Alewell C, Morris CE. 2014 Freezing nucleation apparatus puts new slant on study of biological ice nucleators in precipitation. *Atmos. Meas. Tech.* **7**, 129–134. (doi:10.5194/amt-7-129-2014)

24. Vali G. 1971 Quantitative evaluation of experimental results on the heterogeneous freezing nucleation of supercooled liquids. *J. Atmos. Sci.* **28**, 402–409. (https://doi.org/10.1175/1520-0469(1971)028<0402:QEOERA>2.0.CO;2).

25. Moore JW *et al.* 2015 Emergent stability in a large, free-flowing watershed. *Ecology* **96**, 340–347. (doi:10.1890/14-0326.1)

26. Wagner S, Riedel T, Niggemann J, Vähätalo AV, Dittmar T, Jaffé R. 2015 Linking the molecular signature of heteroatomic dissolved organic matter to watershed characteristics in World Rivers. *Environ. Sci. Technol.* **49**, 13 798–13 806. (doi:10.1021/acs.est.5b00525)

27. Dzwonkowski B *et al.* 2018 Tracking sea surface salinity and dissolved oxygen on a river-influenced, seasonally stratified shelf, Mississippi Bight, northern Gulf of Mexico. *Cont. Shelf Res.* **169**, 25–33. (doi:10.1016/j.csr.2018.09.009)

28. Axson JL, May NW, Colón-Bernal ID, Pratt KA, Ault AP. 2016 Lake spray aerosol: a chemical signature from individual ambient particles. *Environ. Sci. Technol.* **50**, 9835–9845. (doi:10.1021/acs.est.6b01661)

29. McCluskey CS *et al.* 2018 Marine and terrestrial organic ice-nucleating particles inpristine marine to continentally influenced Northeast Atlantic air masses. *J. Geophys. Res. Atmos.* **123**, 6196–6212. (doi:10.1029/2017JD028033)

30. Rosinski J, Haagenson PL, Nagamoto CT, Quintana B, Parungo F, Hoyt SD. 1988 Ice-forming nuclei in air masses over the Gulf of Mexico. *J. Aerosol. Sci.* **19**, 539–551. (doi:10.1016/0021-8502(88)90206-6)

31. Ladino LA *et al.* 2019 Ice-nucleating particles in a coastal tropical site. *Atmos. Chem. Phys.* **19**, 6147–6165. (doi:10.5194/acp-19-6147-2019)

32. Porter GCE *et al.* 2022 Highly active ice-nucleating particles at the summer North Pole. *J. Geophys. Res.* **127**, e2021JD036059. (doi:10.1029/2021JD036059)

33. Creamean JM, Hill TCJ, DeMott PJ, Uetake J, Kreidenweis S, Douglas TA. 2020 Thawing permafrost: an overlooked source of seeds for Arctic cloud formation. *Environ. Res. Lett.* **15**, 084022. (doi:10.1088/1748-9326/ab87d3)

34. Chen J *et al.* 2021 Atmospheric humic-like substances (HULIS) act as ice active entities. *Geophys. Res. Lett.* **48**, e2021GL092443. (doi:10.1029/2021GL092443)

35. O'Sullivan D *et al.* 2014 Ice nucleation by fertile soil dusts: relative importance of mineral and biogenic components. *Atmos. Chem. Phys.* **14**, 1853–1867. (doi:10.5194/acp-14-1853-2014)

36. Suski KJ, Hill TCJ, Levin EJT, Miller A, DeMott PJ, Kreidenweis SM. 2018 Agricultural harvesting emissions of ice-nucleating particles. *Atmos. Chem. Phys.* **18**, 13755–13 771. (doi:10.5194/acp-18-13755-2018)

37. Šantl-Temkiv T, Lange R, Beddows D, Rauter U, Pilgaard S, Dall'Osto M, Gunde-Cimerman N, Massling A, Wex H. 2019 Biogenic sources of ice nucleating particles at the high Arctic site Villum Research Station. *Environ. Sci. Technol.* **53**, 10 580–10 590. (doi:10.1021/acs.est.9b00991)

38. Patade S *et al.* 2021 Empirical formulation for multiple groups of primary biological ice nucleating particles from field observations over Amazonia. *J. Atmos. Sci.* **78**, 2195–2220. (doi:10.1175/JASD-20-0096.1)

39. Chen J, Wu Z, Chen J, Reicher N, Fang X, Rudich Y, Hu M. 2021 Size-resolved atmospheric ice-nucleating particles during East Asian dust events. *Atmos. Chem. Phys.* **21**, 3491–3506. (doi:10.5194/acp-21-3491-2021)

40. Irish VE *et al.* 2017 Ice-nucleating particles in Canadian Arctic sea-surface microlayer and bulk seawater. *Atmos. Chem. Phys.* **17**, 10 583–10 595. (doi:10.5194/acp-17-10583-2017)

41. Irish VE *et al.* 2019 Revisiting properties and concentrations of ice-nucleating particles in the sea surface microlayer and bulk seawater in the Canadian Arctic during summer. *Atmos. Chem. Phys.* **19**, 7775–7787. (doi:10.5194/acp-19-7775-2019)

42. Seidel M, Dittmar T, Ward ND, Krusche AV, Jeffrey ER, Yager PL, Medeiros PM. 2016 Seasonal and spatial variability of dissolved organic matter composition in the lower Amazon River. *Biogeochemistry* **131**, 281–302. (doi:10.1007/s10533-016-0279-4)

43. Joung YS, Ge Z, Buie CR. 2017 Bioaerosol generation by raindrops on soil. *Nat. Commun.* **8**, 14668. (doi:10.1038/ncomms14668)

44. Thoroddsen S, Takehara K, Etoh T. 2012 Micro-splashing by drop impacts. *J. Fluid Mech.* **706**, 560–570. (doi:10.1017/jfm.2012.281)

45. Dunkerley D. 2009 Evaporation of impact water droplets in interception processes: historical precedence of the hypothesis and a brief literature overview. *J. Hydrol.* **376**, 599–604. (doi:10.1016/j.jhydrol.2009.08.004)

46. Dunin FX, O'Loughlin EM, Reyenga W. 1988 Interception loss from eucalypt forest: lysimeter determination of hourly rates for long term evaluation. *Hydrol. Process.* **2**, 315–329. (doi:10.1002/hyp.3360020403)

47. Murakami S. 2006 A proposal for a new forest canopy interception mechanism: splash droplet evaporation. *J. Hydrol.* **319**, 72–82. (doi:10.1016/j.jhydrol.2005.07.002)

48. Huffman JA *et al.* 2013 High concentrations of biological aerosol particles and ice nuclei during and after rain. *Atmos. Chem. Phys.* **13**, 6151–6164. (doi:10.5194/acp-13-6151-2013)

49. Mignani C, Wieder J, Sprenger MA, Kanji ZA, Henneberger J, Alewell C, Conen F. 2021 Towards parameterising atmospheric concentrations of ice-nucleating particles active at moderate supercooling. *Atmos. Chem. Phys.* **21**, 657–664. (doi:10.5194/acp-21-657-2021)

50. Martens CS *et al.* 2004 Radon fluxes in tropical forest ecosystems of Brazilian Amazonia: night-time CO_2 net ecosystem exchange derived from

radon and eddy covariance methods. *Glob. Chang. Biol.* **10**, 618–629. (doi:10.1111/j.1365-2486.2004.00764.x)

51. Whitehead JD *et al.* 2010 Aerosol fluxes and dynamics within and above a tropical rainforest in South-East Asia. *Atmos. Chem. Phys.* **10**, 9369–9382. (doi:10.5194/acp-10-9369-2010)

52. Gabey AM, Gallagher MW, Whitehead J, Dorsey JR, Kaye PH, Stanley WR. 2010 Measurements and comparison of primary biological aerosol above and below a tropical forest canopy using a dual channel fluorescence spectrometer. *Atmos. Chem. Phys.* **10**, 4453–4466. (doi:10.5194/acp-10-4453-2010)

53. Daily MI, Tarn MD, Whale TF, Murray BJ. 2021 The sensitivity of the ice-nucleating ability of minerals to heat and the implications for the heat test for biological ice nucleators. *Atmos. Meas. Tech. Discuss.* **15**, 2635–2665. (https://doi.org/10.5194/amt-15-2635-2022)

54. Bogler S, Borduas-Dedekind N. 2020 Lignin's ability to nucleate ice via immersion freezing and its stability towards physicochemical treatments and atmospheric processing. *Atmos. Chem. Phys.* **20**, 14 509–14 522. (doi:10.5194/acp-20-14509-2020)

55. Pummer BG, Bauer H, Bernardi J, Bleicher S, Grothe H. 2012 Suspendable macromolecules are responsible for ice nucleation activity of birch and conifer pollen. *Atmos. Chem. Phys.* **12**, 2541–2550.

56. Einbock A, Burtscher E, Frey C, Conen F. 2023 Export of ice-nucleating particles from watersheds: results from the Amazon and Tocantins river plumes. Figshare. (doi:10.6084/m9.figshare.c.6405756)